The Neuromedin U-Growth Hormone Secretagogue Receptor 1b/Neurotensin Receptor 1 Oncogenic Signaling Pathway as a Therapeutic Target for Lung Cancer

Koji Takahashi,[1] Chiyuki Furukawa,[1,4] Atsushi Takano,[1] Nobuhisa Ishikawa,[1] Tatsuya Kato,[1] Satoshi Hayama,[1] Chie Suzuki,[1] Wataru Yasui,[2] Kouki Inai,[3] Saburo Sone,[4] Tomoo Ito,[5] Hitoshi Nishimura,[6] Eiju Tsuchiya,[7] Yusuke Nakamura,[1] and Yataro Daigo[1]

[1]Laboratory of Molecular Medicine, Human Genome Center, Institute of Medical Science, The University of Tokyo, Tokyo, Japan; Departments of [2]Molecular Pathology and [3]Pathology, Graduate School of Biomedical Sciences, Hiroshima University, Hiroshima, Japan; [4]Department of Internal Medicine and Molecular Therapeutics, The University of Tokushima School of Medicine, Tokushima, Japan; [5]Department of Surgical Pathology, Hokkaido University Graduate School of Medicine, Sapporo, Japan; [6]Department of Thoracic Surgery, Saitama Cancer Center, Saitama, Japan; and [7]Kanagawa Cancer Center Research Institute, Kanagawa, Japan

Abstract

Using a genome-wide cDNA microarray to search for genes that were specifically up-regulated in non–small cell lung cancers (NSCLC), we identified an abundant expression of neuromedin U (NMU) in the great majority of lung cancers. Immunohistochemical analysis showed a significant association of NMU expression with poorer prognosis of patients with NSCLC. Treatment of NSCLC cells with short interfering RNA against NMU suppressed its expression and inhibited the growth of the cells; on the other hand, the induction of exogenous expression of NMU conferred growth-promoting activity and enhanced cell mobility *in vitro*. We found that two G protein–coupled receptors, growth hormone secretagogue receptor 1b and neurotensin receptor 1, were also overexpressed in NSCLC cells, and that a heterodimer complex of these receptors functioned as an NMU receptor. The NMU-receptor interaction subsequently induced the generation of a second messenger, cyclic AMP, to activate its downstream genes including transcription factors and cell cycle regulators. Treatment of NSCLC cells with short interfering RNAs for growth hormone secretagogue receptor or neurotensin receptor 1 suppressed the expression of those genes and the growth of NSCLC cells. These data strongly implied that targeting the NMU signaling pathway would be a promising therapeutic strategy for the treatment of lung cancers. (Cancer Res 2006; 66(19): 9408-19)

Introduction

Lung cancer is one of the most common causes of cancer death worldwide, and non–small cell lung cancer (NSCLC) accounts for nearly 80% of those cases (1). Many genetic alterations associated with the development and progression of lung cancer have been reported, but the precise molecular mechanisms remain unclear (2). Over the last decade, newly developed cytotoxic agents including paclitaxel, docetaxel, gemcitabine, and vinorelbine have emerged to offer multiple therapeutic choices for patients with advanced NSCLC; however, each of the new regimens can provide only modest survival benefits compared with cisplatin-based therapies (3). Hence, new therapeutic strategies, such as the development of molecular-targeted agents, are eagerly awaited.

Systematic analysis of expression levels of thousands of genes on cDNA microarrays is an effective approach to identifying unknown molecules involved in pathways of carcinogenesis (4–11), and can reveal candidate targets for the development of novel anticancer drugs and tumor markers. We have been attempting to isolate novel molecular targets for the diagnosis, treatment, and prevention of NSCLC by analyzing genome-wide expression profiles of NSCLC cells on a cDNA microarray containing 23,040 genes, after pure populations of tumor cells were prepared from 37 cancer tissues by laser microdissection (4). To verify the biological and clinicopathologic significance of the respective gene products, we have been performing tumor-tissue microarray analysis of clinical lung cancer materials (7–9, 11). In the course of those studies, we observed that the gene encoding neuromedin U (NMU) was frequently overexpressed in primary NSCLCs.

NMU is a neuropeptide that was first isolated from porcine spinal cord. It has potent activity on smooth muscle (12–17), and in mammalian species, NMU is distributed predominantly in the gastrointestinal tract and central nervous system (18, 19). The peripheral activities of NMU include stimulation of smooth muscle, alternation of ion transport in the gut, and regulation of feeding (12); however, any role which NMU might have during lung carcinogenesis has not been implicated. Neuropeptides function peripherally as paracrine and autocrine factors to regulate diverse physiologic processes and act as neurotransmitters or neuromodulators in the nervous system. In general, the receptors which mediate signaling by binding neuropeptides are members of the superfamily of G protein–coupled receptors (GPCR) having seven transmembrane-spanning domains. Two known receptors for NMU, NMU1R and NMU2R, show a high degree of homology to other neuropeptide receptors such as growth hormone secretagogue receptor (GHSR) and neurotensin receptor 1 (NTSR1), for which the corresponding known ligands are ghrelin (GHRL) and neurotensin (NTS), respectively.

In the study reported here, we identified NMU and its downstream molecules as potential targets for the development of novel therapeutic drugs and diagnostic markers. We also show that GHSR1b and NTSR1 could be a cognate heterodimerized receptor complex for NMU, and that this ligand-receptor system significantly affects the growth of lung cancer cells through the

Note: Supplementary data for this article are available at Cancer Research Online (http://cancerres.aacrjournals.org/).

K. Takahashi and C. Furukawa contributed equally to this work.

Requests for reprints: Yataro Daigo, Laboratory of Molecular Medicine, Human Genome Center, Institute of Medical Science, The University of Tokyo, Tokyo 108-8639, Japan. Phone: 81-3-5449-5457; Fax: 81-3-5449-5406; E-mail: ydaigo@ims.u-tokyo.ac.jp.

doi:10.1158/0008-5472.CAN-06-1349

transactivation of its downstream signals involving transcription factors and cell cycle regulators.

Materials and Methods

Cell lines and clinical tissue samples. The 19 human lung cancer cell lines used in this study were as follows: 15 NSCLCs—A549, NCI-H23, NCI-H358, NCI-H522, NCI-H1435, NCI-H1793, LC174, LC176, LC319, PC3, PC9, PC14, SK-LU-1, RERF-LC-AI, and SK-MES-1; and 4 small cell lung cancers (SCLC)—SBC-3, SBC-5, DMS114, and DMS273. All cells were grown in the appropriate medium supplemented with 10% FCS and were maintained at 37°C in an atmosphere of humidified air with 5% CO_2.

Primary NSCLC samples had been obtained earlier with informed consent from 37 patients (4). Fifteen additional primary NSCLCs, including seven adenocarcinomas and eight squamous cell carcinomas, were obtained along with adjacent normal lung tissue samples from patients undergoing surgery at Hokkaido University and its affiliated hospitals (Sapporo, Japan).

A total of 326 formalin-fixed primary NSCLCs (stage I-IIIa) including 224 adenocarcinomas, 86 squamous cell carcinomas, 13 large-cell carcinomas, and 3 adenosquamous carcinomas, and adjacent normal lung tissue samples were obtained from patients who underwent surgery at Hokkaido University and its affiliated hospitals (Sapporo, Japan), and Saitama Cancer Center (Saitama, Japan). Large cell neuroendocrine carcinoma samples from three patients were obtained from the Saitama Cancer Center. Samples of advanced SCLC (stage IV) from postmortem materials (17 individuals) obtained from Hiroshima University (Hiroshima, Japan), were also used in this study. The use of all clinical materials was approved by the Institutional Research Ethics Committees.

Semiquantitative reverse transcription-PCR analysis. Total RNA was extracted from cultured cells and clinical tissues using Trizol reagent (Life Technologies, Inc., Gaithersburg, MD) according to the manufacturer's protocol. Extracted RNAs and normal human tissue polyadenylate RNAs were treated with DNase I (Nippon Gene, Tokyo, Japan) and were reverse-transcribed using oligo$(dT)_{20}$ primer and SuperScript II reverse transcriptase (Invitrogen, Carlsbad, CA). Semiquantitative reverse transcription-PCR (RT-PCR) experiments were carried out with the following synthesized gene-specific primers or with β-actin (*ACTB*)-specific primers as an internal control: *NMU*, 5′-TGAAGAGATTCAGAGTGGACGA-3′ and 5′-ACTGAGAACATTGACAACACAGG-3′; *NMU1R*, 5′-AAGAGGGACAGGGACAAGTAGT-3′ and 5′-ATGCCACTGTTACTGCTTCAG-3′; *NMU2R*, 5′-GGCTCTTACAACTCATGTACCCA-3′ and 5′-TGATACAGAGACATGAAGTGAGCA-3′; *GHSR1a*, 5′-TGGTGTTTGCCTTCATCCT-3′ and 5′-GAATCCCAGAAGTCTGAACA-3′; *GHSR1b*, 5′-CTTGGGACACCAACGAGTG-3′ and 5′-AGGACCCGCGAGAGAAAGC-3′; *NTSR1*, 5′-GGTCTGTGGCTGTGACTGAA-3′ and 5′-GTTTGAGCTGTGAGGGCTGT-3′; *GHRL*, 5′-TGAGCCCTGAACACCAGAGAG-3′ and 5′-AAAGCCAGATGAGCGCTTCTA-3′; *NTS*, 5′-TCTTCAGCATGATGTGTTGTGT-3′ and 5′-TGAGAGATTCATGAGGAAGTCTTG-3′; *FOXM1*, 5′-CCCTGACAACATCAACTGGTC-3′ and 5′-GTCCACCTTCGCTTTTATTGAGT-3′; unannotated transcript (clone IMAGE:3839141, mRNA), 5′-AAAAAGGGGATGCCTAGAACTC-3′ and 5′-CTTTCAGCACGTCAAGGACAT-3′; *GCDH*, 5′-ACACCTACGAAGGTACACATGAC-3′ and 5′-GCTATTTCAGGGTAAATGGAGTC-3′; *CDK5RAP1*, 5′-CAGAGATGGAGGATGTCAATAAC-3′ and 5′-CATAGCAGCTTTAAAGAGACACG-3′; *LOC134145*, 5′-CCACCATAACAGTGGAGTGGG-3′ and 5′-CAGTTACAGGTGTATGACTGGGAG-3′; *NUP188*, 5′-CTGAATACAACTTCCTGTTTGCC-3′ and 5′-GACCACAGAATTACCAAAACTGC-3′; *ACTB,* 5′-GAGGTGATAGCATTGCTTTCG-3′ and 5′-CAAGTCAGTGTACAGGTAAGC-3′. PCR reactions were optimized for the number of cycles to ensure product intensity within the logarithmic phase of amplification.

Northern blot analysis. Human multiple-tissue blots (BD Biosciences Clontech, Palo Alto, CA) were hybridized with a ^{32}P-labeled PCR product of *NMU*. The full-length cDNA of *NMU* was prepared by RT-PCR using primers 5′-CGCGGATCCGCGATGCTGCGAACAGAGAGCTG-3′ and 5′-CCGCTCGAGCGGAATGAACCCTGCTGACCTTC-3′. Prehybridization, hybridization, and washing were done according to the supplier's recommendations. The blots were autoradiographed with intensifying screens at room temperature for 72 hours.

Western blotting. Cells were lysed with radioimmunoprecipitation assay buffer [50 mmol/L Tris-HCl (pH 8.0), 150 mmol/L NaCl, 1% NP40, 0.5% deoxychorate-Na, 0.1% SDS] containing Protease Inhibitor Cocktail Set III (Calbiochem, Darmstadt, Germany). Protein samples were separated by SDS-polyacrylamide gels and electroblotted onto Hybond-ECL nitrocellulose membranes (GE Healthcare Bio-Sciences, Piscataway, NJ). Blots were incubated with a rabbit polyclonal anti-NMU antibody (generated to recombinant NMU), mouse monoclonal anti-FLAG M2 antibody (Sigma-Aldrich, Co., St. Louis, MO), goat polyclonal anti-NTSR1 antibody (Santa Cruz Biotechnology, Inc., Santa Cruz, CA), and rabbit polyclonal anti-GHSR antibody (generated to the peptide GVEHENGTDPWDTNEC). Antigen-antibody complexes were detected using secondary antibodies conjugated to horseradish peroxidase (GE Healthcare Bio-Sciences). Protein bands were visualized by enhanced chemiluminescence Western blotting detection reagents (GE Healthcare Bio-Sciences).

Immunohistochemistry and tissue microarray. To investigate the presence of NMU, GHSR1b, NTSR1, or FOXM1 protein in clinical samples (normal lung tissues, NSCLCs, and SCLCs that had been embedded in the paraffin block), we stained the sections using ENVISION+ Kit/horseradish peroxidase (DakoCytomation, Glostrup, Denmark). Briefly, each polyclonal antibody to NMU, GHSR1b (generated to the peptide GGSQRALRLSLAGPILSLC), NTSR1, or FOXM1 (Santa Cruz Biotechnology) was added after blocking endogenous peroxidase and proteins, and the sections were incubated with horseradish peroxidase–labeled anti-rabbit IgG and anti-goat IgG as the secondary antibody. Substrate chromogen was added and the specimens were counterstained with hematoxylin.

The tumor tissue microarrays were constructed as published previously (20, 21). The tissue area for sampling was selected based on a visual alignment with the corresponding H&E-stained section on a slide. Three-, four-, or five-tissue cores (diameter, 0.6 mm; height, 3-4 mm) taken from the donor tumor blocks were placed into a recipient paraffin block using a tissue microarrayer (Beecher Instruments, Sun Prairie, WI). A core of normal tissue was punched from each case. Five-micrometer sections of the resulting microarray block were used for immunohistochemical analysis. NMU positivity was assessed according to staining intensity as absent (no visible staining in tumor cells) or positive (dark brown staining in >50% of tumor cells completely obscuring cytoplasm) by three independent investigators without prior knowledge of the clinical follow-up data. The intensity of GHSR1b or NTSR1 staining was evaluated as well using the following criteria: positive, dark brown staining in >50% of tumor cells completely obscuring membrane and cytoplasm; absent, no appreciable staining in tumor cells. The intensity of FOXM1 staining was evaluated using the following criteria: positive, dark brown staining in >50% of tumor cells completely obscuring nucleus and cytoplasm; absent, no appreciable staining in tumor cells. Cases were accepted only as positive if reviewers independently defined them as such.

Statistical analysis. Tumor-specific survival curves were calculated from the date of surgery to the time of death related to NSCLC, or to the last follow-up observation. Kaplan-Meier curves were calculated for each relevant variable; differences in survival times among patient subgroups were analyzed using the log-rank test. Univariate and multivariate analyses were done using Cox's proportional hazard regression model to determine associations between clinicopathologic variables and cancer-related mortality. $P < 0.05$ were considered statistically significant.

Immunocytochemical analyses. Cultured cells were washed twice with PBS(−), fixed in 4% paraformaldehyde solution for 60 minutes at room temperature, and rendered permeable with PBS(−) containing 0.1% Triton X-100 for 1.5 minutes. Prior to the primary antibody reaction, cells were covered with blocking solution (3% bovine serum albumin (BSA) in PBS(−)) for 60 minutes to block nonspecific antibody binding. Then the cells were incubated with antibodies to human NMU protein. Antibodies were stained with a goat anti-rabbit secondary antibody conjugated to rhodamine (Cappel, Durham, NC) for revealing endogenous NMU, and viewed with a microscope (DP50; Olympus, Tokyo, Japan).

RNA interference assay. We had previously established a vector-based RNA interference (RNAi) system, psiH1BX3.0, to direct the synthesis of short interfering RNAs (siRNA) in mammalian cells (6, 7, 10, 11). We transfected

10 μg of siRNA expression vector, using 30 μL of LipofectAMINE 2000 (Invitrogen), into NSCLC cell lines A549 and LC319, both of which overexpressed *NMU, GHSR1b, NTSR1*, and *FOXM1* endogenously. The transfected cells were cultured for 5 days in the presence of appropriate concentrations of geneticin (G418), after which, cell numbers and viability were measured by Giemsa staining and triplicate 3-(4,5-dimethylthiazol-2-yl)-2,5-diphenyltetrazolium bromide (MTT) assays. The target sequences of the synthetic oligonucleotides for RNAi were as follows: control 1 [*EGFP*: enhanced green fluorescent protein gene, a mutant of *Aequorea victoria* green fluorescent protein], 5′-GAAGCAGCACGACTTCTTC-3′; control 2 (Luciferase: *Photinus pyralis* luciferase gene), 5′-CGTACGCGGAATACTTCGA-3′; control 3 (Scramble: chloroplast *Euglena gracilis* gene coding for 5S and 16S rRNAs), 5′-GCGCGCTTTGTAGGATTCG-3′; siRNA-NMU (si-*NMU*), 5′-GAGATTCAGAGTGGACGAA-3′; siRNA-GHSR-1 (si-*GHSR-1*), 5′-CCTCTACCTGTCCAGCATG-3′; siRNA-GHSR-2 (si-*GHSR-2*), 5′-GCTGGTCATCTTCGTCATC-3′; siRNA-NTSR1-1 (si-*NTSR1-1*), 5′-GTTCATCAGCGCCATCTGG-3′; siRNA-NTSR1-2 (si-*NTSR1-2*), 5′-GGTCGTCATACAGGTCAAC-3′. To validate our RNAi system, individual control siRNAs (EGFP, Luciferase, and Scramble) were initially confirmed using semiquantitative RT-PCR to decrease the expression of the corresponding target genes that had been transiently transfected into COS-7 cells. Down-regulation of *NMU, GHSR1b*, and *NTSR1* expression by their respective siRNAs (si-*NMU*, si-*GHSR-1*, si-*NTSR1-1*, and si-*NTSR1-2*), but not by controls, was confirmed with semiquantitative RT-PCR in the cell lines used for this assay.

NMU-expressing COS-7 transfectants. NMU-expressing stable transfectants were established according to a standard protocol. The entire coding region of *NMU* was amplified by RT-PCR using the primer sets described above. The product was digested with *Bam*HI and *Xho*I, and cloned into appropriate sites of a pcDNA3.1-myc/His A(+) vector (Invitrogen) that contained c-myc-His-epitope sequences (LDEESILKQEHHHHHH) at the COOH-terminal of the NMU protein. Using FuGENE 6 Transfection Reagent (Roche Diagnostics, Basel, Switzerland) according to the manufacturer's instructions, we transfected COS-7 cells, which do not express endogenous NMU, with plasmids expressing either *NMU* (pcDNA3.1-*NMU*-myc/His), an antisense strand of *NMU* (pcDNA3.1-antisense), or mock plasmids (pcDNA3.1). Transfected cells were cultured in DMEM containing 10% FCS and geneticin (0.4 mg/mL) for 14 days; then 50 individual colonies were trypsinized and screened for stable transfectants by a limiting-dilution assay. Expression of NMU was determined in each clone by RT-PCR, Western blotting, and immunostaining.

Cell growth and colony formation assays. COS-7 transfectants that stably expressed NMU were seeded onto six-well plates (5×10^4 cells/well), and maintained in medium containing 10% FCS and 0.4 mg/mL geneticin for 24, 48, 72, 96, 120, and 144 hours. At each time point, cell proliferation was evaluated by the MTT assay using Cell Counting Kits (Wako, Osaka, Japan). Colonies were counted at 144 hours. All experiments were done in triplicate. Interaction of NMU-25 with COS-7 cells were examined by flow cytometric analysis. Briefly, subconfluent cells were harvested in Cell Dissociation Solution (Sigma-Aldrich) and suspended in DMEM. Then, 1×10^6 cells/microtube were washed with assay buffer [PBS(−) with 10 mmol/L $MgCl_2$, 2 mmol/L EDTA, and 0.1% BSA], and the cells were incubated with 0.5 to 10 μmol/L of rhodamine-labeled NMU-25 peptide (NMU-25-rhodamine; Phoenix Pharmaceuticals, Inc., Belmont, CA) in assay buffer for 2 hours at room temperature. Subsequently, the cells were washed twice with assay buffer. To detect the population of cells binding to rhodamine-labeled NMU-25, flow cytometry was done using a Becton Dickinson FACSCalibur and analyzed by Cell Quest software.

Ligand receptor binding assay. To confirm binding of NMU-25 to the endogenous candidate receptors on the NSCLC cells, we did a receptor-ligand binding assay using the LC319 and PC14 cells that expressed GHSR1b and NTSR1, but did not express NMU1R and NMU2R. Briefly, the trypsinized cells were seeded onto 96-well (with a black wall and clear bottom) microtiter plates 24 hours prior to the assay. The medium was removed and the cells were incubated with Cy5-labeled NMU-25 peptide (1 μmol/L) with or without a 10-fold excess of unlabeled NMU-25 peptide as a competitor. The plate was incubated in the dark for 24 hours at 37°C and was then scanned on the 8200 Cellular Detection System (Applied Biosystems, Foster City, CA) to quantify the amount of Cy5 fluorescence probe bound to the surface of each cell.

Immunocytochemistry for internalized receptors. To investigate the association of NMU-25 with its candidate receptors, GHSR1b and NTSR1, we did the following experiments. The entire coding region of each receptor gene was amplified by RT-PCR using primers *GHSR1b* (5′-GGAATTCCATGTGGAACGCGACGCCCAGCGAA-3′ and 5′-CGCGGATCCGCGGAGAGAAGGGAGAAGGCACAGGGA-3′) and *NTSR1* (5′-GGAATTCCATGCGCCTCAACAGCTCCGCGCCGGGAA-3′ and 5′-CGCGGATCCGCGGTACAGCGTCTCGCGGGTGGCATTGCT-3′). The products were digested with *Eco*RI and *Bam*HI and cloned into appropriate sites of p3XFLAG-CMV10 vector (Sigma-Aldrich). We transfected COS-7 cells with FLAG-tagged GHSR1b or NTSR1 expression plasmids using FuGENE 6 Transfection Reagent, as described above. The cells subjected to internalization assays were exposed to NMU-25 (10 μmol/L) for 120 minutes. Cells were then fixed with 4% paraformaldehyde solution for 15 minutes at 37°C, and washed with PBS(−). Specimens were incubated in PBS(−) containing 0.1% Triton X-100 for 10 minutes and subsequently washed with PBS(−). Prior to the primary antibody reaction, cells were incubated in CAS-BLOCK (Zymed Laboratories, Inc., South San Francisco, CA) for 10 minutes to block nonspecific antibody binding. Then the cells were incubated with both rabbit polyclonal anti-GHSR antibody and goat polyclonal anti-NTSR1 antibody. Antibodies were stained with both anti-rabbit secondary antibody conjugated to Alexa Fluor 488 (Molecular Probes, Eugene, OR) and anti-goat secondary antibody conjugated to Alexa Fluor 594 (Molecular Probes). DNA was stained with 4′,6-diamidino-2-phenylindole (DAPI). Images were viewed and assessed using a confocal microscopy (TCS SP2 AOBS; Leica Microsystems, Wetzlar, Germany).

Internalization study with fluorescence ligand of NMU. LC319 cells were grown in DMEM containing 10% FCS. The cells were washed in PBS(−), and preincubated for 10 minutes at 37°C in DMEM containing 0.1% BSA. They were then incubated for various periods of time with Alexa Fluor 594–labeled NMU-25 peptide in DMEM containing 0.1% BSA. At the end of the incubation, the cells were washed thrice with ice-cold PBS(−), fixed with 4% paraformaldehyde solution, initially for 5 minutes on ice, and then for 15 minutes at room temperature. The cells were washed and treated with DAPI. Images were viewed and assessed using a confocal microscopy (TCS SP2 AOBS; Leica Microsystems). Optical sections with intervals of 0.25 μm were taken with a 63×/1.4 objective.

Detection of receptor dimerization. Cultured cells were washed twice with ice-cold PBS(−) and incubated with 5 mmol/L dithiobis[succinimidyl-propionate] (Pierce, Rockford, IL) for 60 minutes in PBS(−) on ice. The reaction was quenched by incubation with Stop solution [1 mol/L Tris (pH 7.5)] in a final concentration of 50 mmol/L Tris for 15 minutes on ice. Cells were then washed twice with ice-cold PBS(−) and lysed in ice-cold Tx/G buffer [300 mmol/L NaCl, 1% Triton X-100, 10% glycerol, 1.5 mmol/L $MgCl_2$, 1 mmol/L $CaCl_2$, and 10 mmol/L iodoacetamide in 50 mmol/L Tris-Cl (pH 7.4)] containing protease inhibitor (Protease Inhibitor Cocktail Set III; Calbiochem) for 60 minutes on ice. Iodoacetamide was included in each buffer used for protein preparation to prevent nonspecific disulfide linkages. The lysates were then centrifuged for 15 minutes at 15,000 rpm at 4°C, and the supernatants were incubated with anti-FLAG M2-agarose affinity beads (Sigma-Aldrich) at 4°C overnight. The immunoprecipitates (containing cell surface receptors) were collected, washed thrice with TBST buffer [150 mmol/L NaCl, 0.05% Tween 20 in 20 mmol/L Tris-Cl (pH 7.6)], and eluted in non–reducing Laemmli sample buffer. The solutions were subjected to SDS-PAGE, and receptor proteins were detected by Western blot analysis using a mouse monoclonal anti-FLAG M2 antibody, goat polyclonal anti-NTSR1 antibody, or rabbit polyclonal anti-GHSR antibody as a primary antibody, and rec-Protein G-Peroxidase Conjugate (Zymed Laboratories) to detect antigen-antibody complexes.

Measurement of cyclic AMP levels. Trypsinized LC319 cells were seeded onto 96-well microtiter plate (5.0×10^4 cells) and cultured in appropriate medium supplemented with 10% FCS for 24 hours, and then the medium was changed to serum-free/1 mmol/L of 3-isobutyl-1-methylxanthine 20 minutes prior to the assay. Next, cells were incubated with individual concentrations of peptides (NMU-25, GHRL, or NTS) for

20 minutes and their cyclic AMP (cAMP) levels were measured using the cAMP EIA System (GE Healthcare Bio-Sciences).

Identification of downstream genes of NMU by cDNA microarray. LC319 cells were transfected with either siRNA against *NMU* (si-*NMU*) or Luciferase (LUC; control siRNA). mRNAs were extracted 0, 6, 12, 24, 36, 48, and 60 hours after the transfection, labeled with Cy5 or Cy3 dye, and subjected to cohybridization onto cDNA microarray slides containing 32,256 genes as described (5). After normalization of the data, genes with signals higher than the cutoff value were analyzed further. Genes whose intensity was significantly decreased in accordance with the reduction of *NMU* expression were initially selected using self-organizing map cluster analysis (22). Validation of candidate downstream genes of NMU was done using semiquantitative RT-PCR experiments of the same mRNAs from LC319 cells used for microarray hybridization, with gene-specific primers.

Results

NMU in lung tumors and normal tissues. To search for novel target molecules for the development of therapeutic agents and/or diagnostic biomarkers for NSCLC, we first screened genes that showed 5-fold higher expression in >50% of 37 NSCLCs analyzed by cDNA microarray. Among the 23,040 genes screened, we identified the *NMU* transcript to be frequently overexpressed in these NSCLCs and confirmed increased *NMU* expression in the majority of additional NSCLC cases (Fig. 1*A*). In addition, we observed the up-regulation of *NMU* in 13 of 15 NSCLC cell lines and in all 4 SCLC cell lines examined (Fig. 1*B*). Using immunoblot analyses, we subsequently confirmed the expression of NMU protein in lung cancer tissues and cell lines. Western blot analysis revealed an increased NMU protein expression in tumor tissues from the representative pairs of NSCLC samples analyzed (Supplementary Fig. S1*A*). We also found increased NMU protein expression in lung cancer cell lines (Supplementary Fig. S1*B*); the results were consistent with the RT-PCR data (Fig. 1*B*). Northern blotting with *NMU* cDNA as a probe identified a 0.8 kb transcript as a very weak band only in brain and stomach among the 15 normal human tissues examined (data not shown). We also examined NMU expression in clinical lung cancers using tissue microarray system. Positive staining (dark brown staining in >50% of tumor cells completely obscuring the cytoplasm) was observed in 68% of surgically resected NSCLCs (220 of 326) and 82% of SCLCs (14 of 17), whereas no staining was observed in any of normal lung tissues examined (Fig. 1*C*). Positive staining was also observed in all of three large cell neuroendocrine carcinomas. The positive signal by anti-NMU antibody obtained in lung cancer tissues was completely diminished by preincubation of the antibody with recombinant human NMU, indicating its high specificity to NMU protein (Supplementary Fig. S1*C*). We found that patients with NSCLC with NMU-positive tumors showed shorter survival times than patients whose tumors were negative for NMU (P = 0.0363 by the log-rank test; Fig. 1*D*). By univariate analysis, pT (T_1 versus $T_{2\text{-}4}$), pN (N_0 versus $N_{1\text{-}2}$), age (<65 versus ≥65), gender (female versus male), and NMU expression (negative versus positive) were all significantly related to poor survival among patients with NSCLC (P = 0.0012, < 0.0001, 0.0024, 0.0237, and 0.0379, respectively). In multivariate analysis of the prognostic factors, only pT stage, pN stage, gender, and age were indicated to be an independent prognostic factor (P = 0.0011, < 0.0001, 0.0495, and 0.0007, respectively), whereas NMU expression could not be an independent factor (P = 0.0909), thus suggesting the relevance of NMU expression in tumor cells to these clinicopathologic factors.

Effect of NMU on the growth of NSCLC cells. To assess whether NMU is essential for the growth or survival of lung cancer cells, we

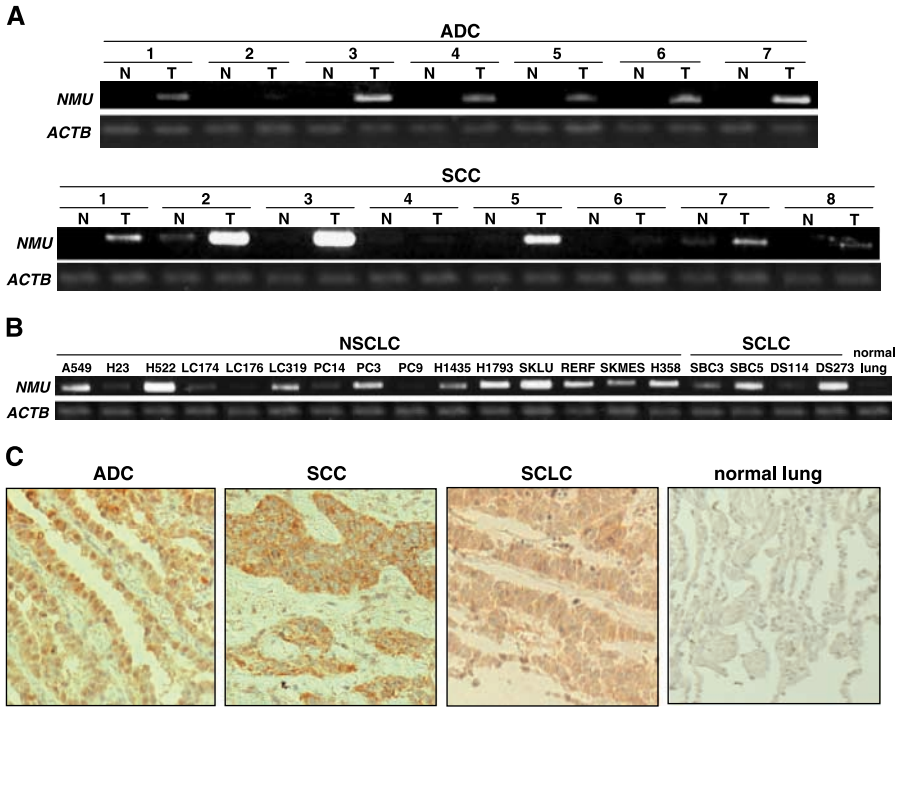

Figure 1. NMU expression in primary lung cancers and cell lines. *A,* expression of *NMU* in clinical samples of NSCLC (*T*) and corresponding normal lung tissues (*N*), examined by semiquantitative RT-PCR. *B,* expression of *NMU* in lung cancer cell lines. *C,* immunohistochemical staining of representative surgically resected and autopsy samples including NSCLC [lung adenocarcinoma (ADC) and squamous cell carcinoma (SCC)] and SCLC as well as normal lung, using anti-NMU antibody on tissue microarrays (original magnification, ×200). *D,* Kaplan-Meier analysis of tumor-specific survival in patients with NSCLC according to NMU expression (P = 0.0363 by the log-rank test).

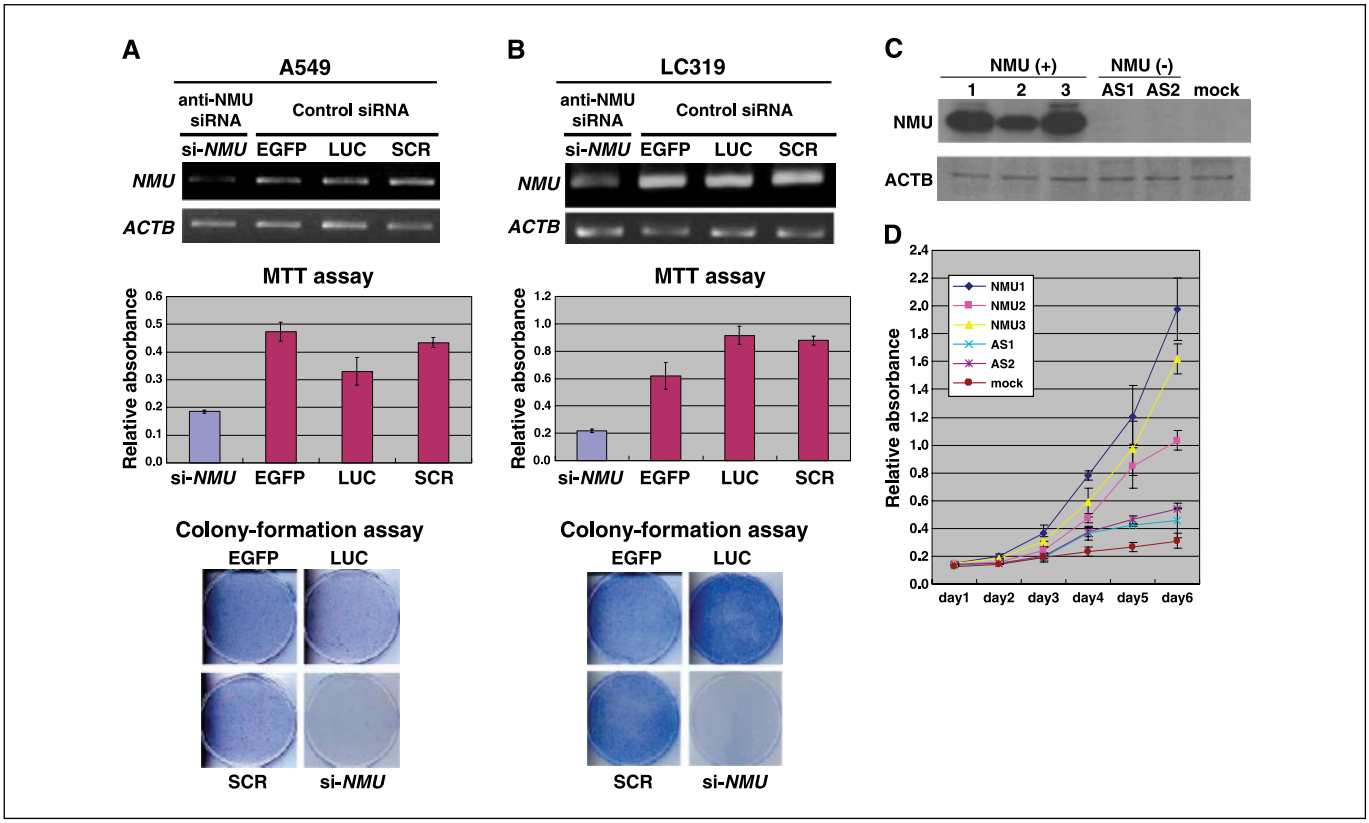

Figure 2. Growth effect of NMU. *A* and *B,* expression of *NMU* in response to si-*NMU* or control siRNAs (EGFP, LUC, or SCR) in A549 (*A*) and LC319 (*B*) cells, analyzed by semiquantitative RT-PCR (*A* and *B, top*). Viability of A549 or LC319 cells evaluated by MTT assay in response to si-NMU, -EGFP, -LUC, or -SCR (*A* and *B, middle*). Colony formation assays of A549 and LC319 cells transfected with specific siRNAs or control plasmids (*A* and *B, bottom*). All experiments were done in triplicate. *C* and *D,* effect of NMU on the growth of COS-7 cells. Expression of NMU in stable transfectants of COS-7 cells on Western blots (*C*). Three independent transfectants expressing high levels of NMU (COS-7-NMU-1, -2, and -3) and controls (COS-7-AS1, -AS2, and mock) were each cultured in triplicate; at each time point, the cell viability was evaluated by the MTT assay (*D*).

designed and constructed plasmids to express siRNA against *NMU* (si-*NMU*), and three different control plasmids [siRNAs for EGFP, Luciferase (LUC), or Scramble (SCR)], and transfected them into A549 (Fig. 2*A*) and LC319 (Fig. 2*B*) cells to suppress the expression of endogenous *NMU*. The amount of *NMU* transcript in the cells transfected with si-*NMU* was significantly decreased in comparison with cells transfected with any of the three control siRNAs (Fig. 2*A* and *B, top*); transfection of si-*NMU* also resulted in significant decreases in cell viability and colony numbers measured by MTT and colony formation assays (Fig. 2*A* and *B, middle* and *bottom*).

Autocrine growth-promoting effect of NMU. To disclose the potential role of NMU in tumorigenesis, we prepared plasmids designed to express either *NMU* (pcDNA3.1-*NMU*-myc/His) or a complementary strand of *NMU* (pcDNA3.1-antisense). We transfected each of these two plasmids into COS-7 cells and confirmed the expression of NMU protein in cytoplasm and Golgi structures by immunocytochemical staining using anti-NMU antibody (data not shown).

To determine the effect of NMU on the growth of mammalian cells, we carried out a colony formation assay of COS-7-derived transfectants that stably expressed NMU. Immunocytochemical analysis using anti-NMU antibody detected NMU protein in >90% of the COS-7 cells in the culture (Supplementary Fig. S2*A*). We established three independent COS-7 cell lines expressing exogenous NMU (COS-7-NMU-1, -2, and -3; Fig. 2*C*), and compared their growth with control cells transfected with antisense strand or mock vector (COS-7-AS-1 and -2; COS-7-mock). Growth of all of the three COS-7-NMU cells was promoted at a significant degree in accordance with the expression level of NMU (Fig. 2*D*). There was also a remarkable tendency in COS-7-NMU cells to form larger colonies than the control cells (Supplementary Fig. S2*B*). Furthermore, we did colony formation assays to investigate whether the NMU could act as a growth-promoting factor for lung-cancer cells (LC319). The number of geneticin-resistant colonies was significantly increased in dishes containing LC319 cells that had been transfected with the sense strand of cDNA (pcDNA3.1-*NMU*-myc/His) corresponding to the normal transcript, in comparison to cells transfected with the mock vector (Supplementary Fig. S2*C*).

As the immunohistochemical analysis on tissue microarray had indicated that lung cancer patients with NMU-positive tumors showed shorter cancer-specific survival periods than patients whose tumors were negative for NMU, we did Matrigel invasion assays using COS-7-NMU cells. Invasion of COS-7-NMU cells through Matrigel was significantly enhanced, compared with the control cells transfected with mock plasmids, suggesting that NMU could also contribute to the highly malignant phenotype of lung cancer cells (Supplementary Fig. S2*D*).

Subsequently, we carried out autocrine assays using the active form of a 25–amino acid polypeptide of commercially available NMU (NMU-25). To investigate whether NMU-25 would affect cell growth, we incubated COS-7 cells with either NMU-25 or BSA (control) at final concentrations of 0.3 to 15 μmol/L in the culture medium. COS-7 cells incubated with NMU-25 showed enhancement of the cell

growth by MTT and colony formation assays, compared with the control, in a dose-dependent manner (Fig. 3*A* and *B*). We also detected by flow cytometry that rhodamine-labeled NMU-25 peptide bound to the surface of COS-7 cells in a dose-dependent manner (Fig. 3*C*). The results suggested that the growth-promoting effect of NMU was likely to be mediated through binding of NMU-25 to a receptor(s) on the cell surface of COS-7. Subsequently, we investigated whether anti-NMU antibody (0.5-7.5 μmol/L) could inhibit the growth of COS-7 cells cultured in medium containing 3 μmol/L of NMU-25. Expectedly, growth enhancement caused by the addition of 3 μmol/L of NMU-25 was neutralized by the 7.5 μmol/L concentration of anti-NMU antibody, and the viability of COS-7 cells became almost equivalent to that of cells cultured without NMU-25 (Fig. 3*D*).

We then investigated the effect of anti-NMU antibody (0.5-7.5 μmol/L) on the growth of two lung cancer cell lines, LC319 and A549, which showed high levels of endogenous *NMU* expression. The growth of both lines were suppressed by the addition of anti-NMU antibody into their culture media, in a dose-dependent manner ($P < 0.0001$, $P = 0.0002$, respectively; each paired t test), whereas that of LC176 cells expressing NMU at a hardly detectable level was not affected (Supplementary Fig. S3). These data indicated that NMU functions as an autocrine/paracrine growth factor for the proliferation of NSCLC cells.

GHSR1b/NTSR1 as receptors for NMU in a growth-promoting pathway. Two known NMU receptors, NMU1R (FM3/GPR66) and NMU2R (FM4), play important roles in energy homeostasis (17–19). NMU1R is present in many peripheral human tissues (17–19), but NMU2R is only located in the brain. To investigate whether *NMU1R* and *NMU2R* genes were expressed in NSCLCs and whether it is responsible for the growth-promoting effect, we analyzed the expression of these NMU receptors in normal human brain and lung, in NSCLC cell lines, and in clinical tissues by semiquantitative RT-PCR experiments. Neither *NMU1R* nor *NMU2R* expression was detected in any of the lung cancer cell lines or clinical cancer samples examined, although *NMU1R* was expressed in the lung and *NMU2R* in the brain (data not shown), suggesting that NMU is likely to mediate its growth-promoting effect through interaction with other receptor(s) in lung cancer cells.

NMU1R and NMU2R were originally isolated as homologues of known neuropeptide GPCRs. We speculated that unidentified NMU receptor(s) having some degree of homology to NMU1R/NMU2R would be involved in the signaling pathway and searched for candidate NMU receptors using the BLAST program. The homology and expression patterns of genes in NSCLCs in our expression profile data picked up GHSR1b and NTSR1 as good candidates. GHSR has two transcripts, types 1a and 1b. The human GHSR type 1a cDNA encodes a predicted polypeptide of 366 amino acids with seven transmembrane domains, a typical feature of G protein–coupled receptors. A single intron separates its open reading frame into two exons encoding transmembrane domains 1 to 5 and 6 to 7, placing GHSR1a into the intron-containing class of GPCRs. Type 1b is a nonspliced mRNA variant transcribed from a single exon that encodes a polypeptide of 289 amino acids with five transmembrane domains. Our semiquantitative RT-PCR analysis using specific primers for each variant indicated that *GHSR1a* was not expressed in NSCLCs. On the other hand, *GHSR1b* and *NTSR1* were expressed at a relatively high level in some NSCLC cell lines, but not in normal lung (Fig. 4*A*). The *GHSR1b* product reveals 46% homology to NMU1R, and *NTSR1* encodes 418 amino acids with 47% homology to NMU1R. COS-7 cells examined using the autocrine growth-promoting effect of NMU as described above, were confirmed by semiquantitative RT-PCR analysis to endogenously express both *GHSR1b* and *NTSR1* (data not shown). Furthermore, we did immunohistochemical analysis with anti-GHSR1b and anti-NTSR1 polyclonal antibodies using tissue microarrays consisting of 326 NSCLC tissues. Of the 326 cases, GHSR1b staining was positive for 218 (67%; Fig. 4*B, top*), and 217 cases were positive for NTSR1 (67%; Fig. 4*B, bottom*). The expression pattern of GHSR1b or NTSR1 was significantly concordant with NMU expression in these tumors ($\chi^2 = 68$ and 79; $P < 0.0001$ and <0.0001, respectively).

To investigate the binding of NMU-25 to the endogenous GHSR1b and NTSR1 on the NSCLC cells, we did receptor-ligand binding assay using LC319 and PC14 cells treated with NMU-25 (1 μmol/L). We detected binding of Cy5-labeled NMU-25 to the surface of these two cell lines that had endogenously expressed both novel candidate receptors (GHSR1b and NTSR1), but expressed no detectable NMU1R/NMU2R (Fig. 4*A*). The binding activity was elevated in a dose-dependent manner (data not

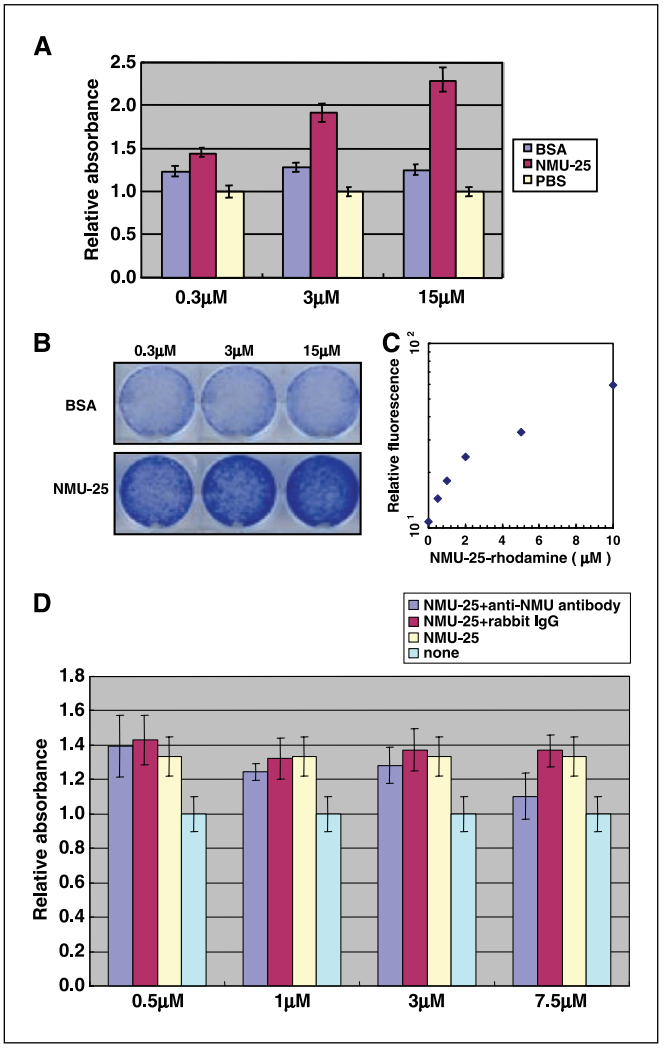

Figure 3. Autocrine effect of NMU on growth of mammalian cells. *A* and *B,* cell viability (*A*) and numbers (*B*) counted by MTT and colony formation assays (COS-7 cells treated with NMU-25 in final concentrations of 0.3-15 μmol/L). *C,* flow cytometric analysis detecting the levels of rhodamine-labeled NMU-25 peptide bound to the surface of COS-7 cells (0-10 μmol/L; *y* axis). *D,* MTT assay evaluating the competitive-binding effect of anti-NMU antibody (0.5-7.5 μmol/L; *y* axis) on the activity of NMU-25 peptide (3 μmol/L) in the culture medium of COS-7 cells.

shown) and was inhibited by the addition of a 10-fold excess of unlabeled NMU-25 as a competitor (Fig. 4*C, top* and *bottom*), suggesting the specific interaction of NMU-25 to these cells.

Biologically active ligands for GPCRs have been reported to bind specifically to their cognate receptors and cause an increase in second messengers such as intracellular-Ca^{2+} and/or cAMP levels. We therefore determined the ability of NMU for the induction of these second messengers in LC319 cells through its interaction with GHSR1b/NTSR1. Enhancement of cAMP production (Fig. 4*D*), but not of Ca^{2+} flux, was detected by NMU-25 in a dose-dependent manner in LC319 cells that expressed both GHSR1b and NTSR1, when the cells were cultured in the presence of NMU-25 in final concentrations of 3 to 100 μmol/L in the culture media (data not shown). The results showed that NMU-25 activated the NMU-25-related signaling pathway possibly through functional GHSR1b/NTSR1 in NSCLC cells. This effect was likely to be NMU-25-specific, because the addition of the same amount of GHRL and NTS, known ligands for GHSR/NTSR1, did not enhance cAMP production (Fig. 4*D*). On the other hand, treatment with NTS, but not that with GHRL, caused the mobilization response of intracellular Ca^{2+} in LC319 cells (data not shown), similar to previous reports (23, 24), suggesting the ligand-dependent and diverse physiologic function of GHSR1b and/or NTSR1 in mammalian cells.

We then examined the biological significance of the NMU-receptor interaction in pulmonary carcinogenesis using plasmids designed to express siRNA against *GHSR* or *NTSR1* (si-*GHSR-1,* si-*NTSR1-1*, and si-*NTSR1-2*). Transfection of either of these plasmids into LC319 or A549 cells suppressed the expression of the endogenous receptor in comparison with cells containing any of the three control siRNAs (Supplementary Fig. S4, *top*). In accordance with the reduced expression of the receptors, LC319 and A549 cells showed significant decreases in cell viability and number of colonies (Supplementary Fig. S4, *middle* and *bottom*). These results strongly support the possibility that NMU, by interaction with GHSR1b and NTSR1, might play a very significant role in the development/progression of lung cancer.

Internalization of GHSR1b/NTSR1 receptors after binding with NMU. To determine the mechanism involved in the regulation

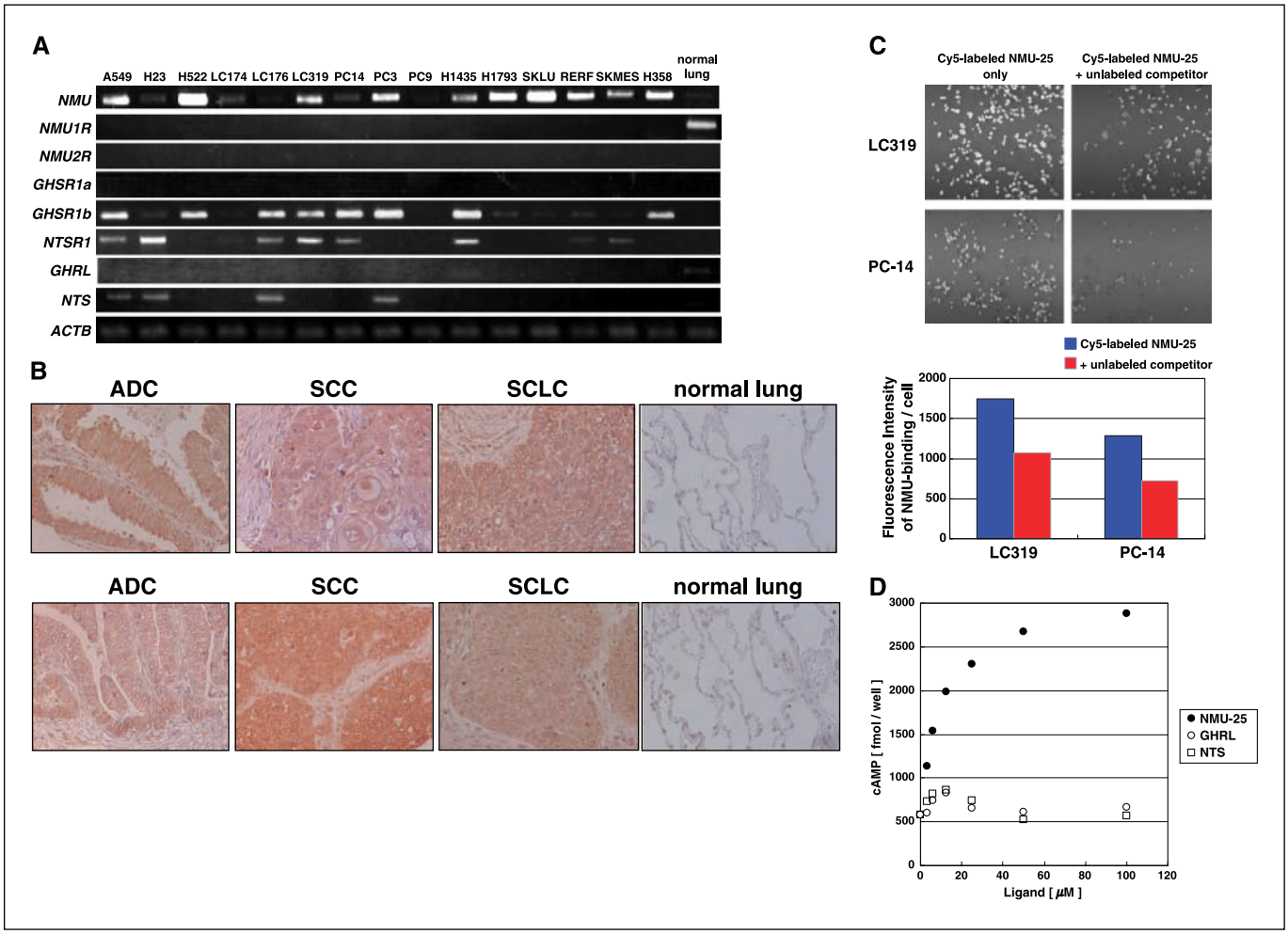

Figure 4. Functional association of NMU with endogenous GHSR1b/NTSR1 on the NSCLC cells. *A,* expression of *NMU*, candidate receptors, and their known ligands as detected by semiquantitative RT-PCR analysis in NSCLC cell lines. *B,* immunohistochemical staining of representative surgically resected and autopsy samples including NSCLC [lung adenocarcinoma (ADC) and squamous cell carcinoma (SCC)] and SCLC as well as normal lung, using anti-NTSR1 (*top*) or anti-GHSR1b (*bottom*) antibody (original magnification, ×200). *C,* binding of Cy5-labeled NMU-25 to the cell surface of NSCLC cells analyzed by laser scanning imaging. Digital fluorescence images of Cy5-labeled NMU-25 (1 μmol/L) bound to LC319 and PC14 cells with/without 10 μmol/L of nonlabeled NMU-25 peptides as a competitor was detected by the 8200 Cellular Detection System (*top*). *Columns,* the average fluorescence values of Cy5-labeled NMU-25 bound to each cell in duplicate assays (*bottom*). *D,* specific signal transduction by NMU as represented by cAMP release in LC319 cells. Dose-response curves of intracellular cAMP production by NMU-25 (●), GHRL (○), or NTS (□) treatment (3-100 μmol/L) in LC319 cells were shown.

of NMU-GHSR1b/NTSR1 signaling, we examined whether GHSR1b/NTSR1 is internalized when they are exposed to NMU, through confocal microscopy observation of the subcellular distribution of the two receptors after NMU-25 stimulation. After they were introduced in COS-7 cells, the GHSR1b and NTSR1 receptors were mainly colocated at the plasma membrane in the condition without the exposure to NMU-25. However, once NMU-25 was added to the cell culture, both of the receptors were cointernalized and predominantly formed the vesicle-like structures in a time-dependent manner (Fig. 5*A*). Similarly, in LC319 cells, in which GHSR1b and NTSR1 were endogenously overexpressed, NMU stimulation induced the cointernalization of the two receptors (Supplementary Fig. S5). The results suggest the possible physical interaction between GHSR1b and NTSR1, as well as NMU-induced cointernalization.

To further confirm whether NMU is internalized after binding to its receptors, internalization of NMU was investigated using Alexa Fluor 594–labeled NMU-25 (NMU-25-Alexa 594) and a confocal microscopy. The binding of agonists to GPCRs on the cell surface is generally known to initiate receptor-mediated endocytosis. In the course of this process, receptors are passed through multiple intracellular pathways that lead to lysosomal degradation or recycling them to the cell surface (25, 26). On the other hand, far less is known about whether all GPCR ligands are internalized together with their receptor. In the case of neuropeptides, the ligand is usually internalized with its receptor (27, 28). As shown in Fig. 5*B*, the *xz*- and *yz*-projections indicated that NMU-25-Alexa 594 was incorporated within the cells. After 15 minutes of incubation, the internalized ligand was concentrated in dots or irregular clusters at more peripheral parts of the cytoplasm in cells (Fig. 5*B, left*). In contrast, after 45 minutes of incubation, fluorescence was concentrated within small spots clustered in the center of the cells, close to the nucleus (Fig. 5*B, right*). These results are similar to the previous reports demonstrating that internalization of NTS proceeded through small endosome-like organelles and the internalized ligand to accumulate at the core of the cell surrounding the nucleus (29).

Functional receptor dimerization of GHSR1b and NTSR1. To examine the direct association between GHSR1b and NTSR1, we transiently expressed either FLAG-tagged GHSR1b or FLAG-tagged NTSR1 individually, and also coexpressed both the FLAG-tagged receptors in COS-7 cells (representative data for GHSR1b was shown in Fig. 5*C*). COS-7 cells were confirmed by semiquantitative RT-PCR analysis to endogenously express both *GHSR1b* and *NTSR1*, but not NMU. Cell lysates preincubated with the cross-linking reagent were immunoprecipitated by anti-FLAG antibody, and were served for Western blot analysis using anti-FLAG, anti-NTSR1, or anti-GHSR antibody. We found coprecipitation of the following proteins: the GHSR1b monomer (~30 kDa), the NTSR1 monomer (~45 kDa), the GHSR1b/NTSR1 heterodimer (~70-75 kDa), the GHSR1b homodimer (~60-65 kDa), and the NTSR1 homodimer (~90-95 kDa; Fig. 5*C*). No such species were detected when empty vector (mock) was transfected to COS-7 cells as a negative control. In the cells expressing only FLAG-tagged NTSR1 and those coexpressing both the FLAG-tagged receptors (NTSR1 and GHSR1b), similar results were observed (data not shown). These results confirm an interaction between GHSR1b and NTSR1, implying the existence of a GHSR1b/NTSR1 heterodimer.

To further confirm the functional importance of the activation and heterodimerization of GHSR1b and NTSR1 at the signal transduction level, we examined the dose-dependent intracellular cAMP production by NMU-25 in lung cancer cell lines representing various expression patterns of the two receptors as detected by semiquantitative RT-PCR analysis (Fig. 5*D*). In LC319 cells expressing high levels of both receptors, treatment with NMU-25 resulted in a marked and reproducible cAMP accumulation (Fig. 5*D, top left*). RERF-LC-AI cells expressing low levels of both receptors, showed significant but low cAMP production in response to NMU-25 (Fig. 5*D, top right*). NCI-H358 and SK-MES-1 cells expressing either of the receptors did not show detectable cAMP production (Fig. 5*D, bottom*).

Identification of downstream genes of NMU. To further elucidate the NMU-signaling pathway, siRNA against *NMU* (si-*NMU*) or LUC (control siRNA) were transfected into LC319 cells overexpressing *NMU*, and genes that were down-regulated in the former cells were screened using a cDNA microarray containing 32,256 genes. By this approach, we selected 70 genes whose expression was significantly decreased in accordance with *NMU* suppression by performing the self-organizing map clustering analysis (22). Semiquantitative RT-PCR analysis confirmed the reduction of candidate transcripts in a time-dependent manner in LC319 cells transfected with si-*NMU*, but not with control siRNA for LUC (Fig. 6*A*). We also evaluated the transactivation of these genes in accordance with the introduction of *NMU* expression in lung cancer cell lines (data not shown) and finally identified six candidate NMU-target genes, *FOXM1, GCDH, CDK5RAP1, LOC134145, NUP188*, and one unannotated transcript (clone IMAGE: 3839141; Fig. 6*B*). Among these six genes selected, *FOXM1* mRNA levels were found to be significantly elevated in clinical cases of lung cancer and showed good concordance with expression levels of *NMU* and two receptors, *GHSR1b* and *NTSR1* (Fig. 6*C*). To validate the induction of the *FOXM1* expression by the NMU ligand-receptor signaling, we cultured LC319 cells expressing GHSR1b and NTSR1 in the presence of NMU-25 or BSA (control) at final concentrations of 25 μmol/L in the culture media, and confirmed an enhanced expression of *FOXM1* in the NMU-treated cells (Fig. 6*D*). Furthermore, we did immunohistochemical analysis of NSCLCs with anti-FOXM1 polyclonal antibodies using tissue microarrays. Of the 325 cases of NSCLC available for this assay, FOXM1 staining was positive for 230 (70.8%; Supplementary Fig. S6*A*). The expression pattern of FOXM1 was significantly concordant with NMU expression in these tumors ($\chi^2 = 68$; $P < 0.0001$). We found that patients with NSCLC with FOXM1-positive tumors showed shorter survival times than patients whose tumors were negative for FOXM1 ($P = 0.0495$ by the log-rank test; Supplementary Fig. S6*B*). These results independently show that NMU, by the interaction with GHSR1b/NTSR1 heterodimer and subsequent activation of its downstream targets, such as *FOXM1*, could significantly affect the growth and malignant nature of lung cancer cells.

Discussion

Recent acceleration in the identification and characterization of novel molecular targets for cancer therapy has stimulated considerable interest in the development of new types of anticancer agents (3). Molecular-targeted drugs are expected to be highly specific to malignant cells, with minimal risk of adverse effects due to their well-defined mechanisms of action. As a promising strategy to identify such molecules, we combined the power of genome-wide expression analysis with high-throughput screening of loss-of-function effects by means of the RNAi technique. In addition, we used tissue microarrays to analyze hundreds of archived clinical samples for validation of the potential target proteins. Using this approach, we have shown here that *NMU* and its cancer-specific receptors, as well as its target genes,

are frequently overexpressed in clinical samples of lung cancer and in cell lines, and that those gene products play indispensable roles in the growth and progression of lung cancer cells.

A COOH-terminal asparaginamide structure and the COOH-terminal heptapeptide core of NMU protein are essential for its contractile activity in smooth muscle cells (30). Recent studies have indicated that NMU acts at the hypothalamic level to inhibit food intake; therefore, this protein might be a physiologic regulator of feeding and body weight (18, 31, 32). NMU was also expressed in several types of human tumors (33–35), but no reports have thus far suggested the involvement of NMU overexpression in pulmonary carcinogenesis, and its precise biological function in cancer cells have never been clarified.

Our treatment of NSCLC cells with specific siRNA to reduce the expression of *NMU* resulted in growth suppression. We also found other evidence supporting the significance of this pathway in carcinogenesis; e.g., the addition of NMU into the medium promoted the growth of COS-7 cells in a dose-dependent manner. The expression of NMU also resulted in the significant promotion of cell growth and invasion in *in vitro* assays. Moreover, clinicopathologic evidence obtained through our tissue microarray experiments showed that NSCLC patients with tumors expressing NMU showed shorter cancer-specific survival periods than those with negative NMU expression. The results obtained by *in vitro* and *in vivo* assays strongly suggested that overexpressed NMU is likely to be an important growth factor and might be associated with cancer cell growth and invasion, functioning in an autocrine manner, and that screening molecules targeting the NMU receptor growth-promoting pathway should be a promising therapeutic approach for treating lung cancers. Because NMU is a secreted protein and most of the clinical NSCLC samples used for our analysis were at an early and operable stage, NMU might also serve as a biomarker for diagnosis of early stage lung cancer, as well as an indicator for a highly malignant phenotype of lung cancer cells, in combination with fiberscopic transbronchial biopsy or blood tests.

NMU was already known to interact with at least two receptors, NMU1R (FM3/GPR66) and NMU2R (FM4), each of which has seven predicted α-helical transmembrane domains containing highly conserved motifs, as do other members of the rhodopsin GPCR family (17–19). The results presented here, however, indicated that these two known receptors were not the targets for the autocrine NMU-signaling pathway in NSCLCs; instead, the *GHSR1b* and

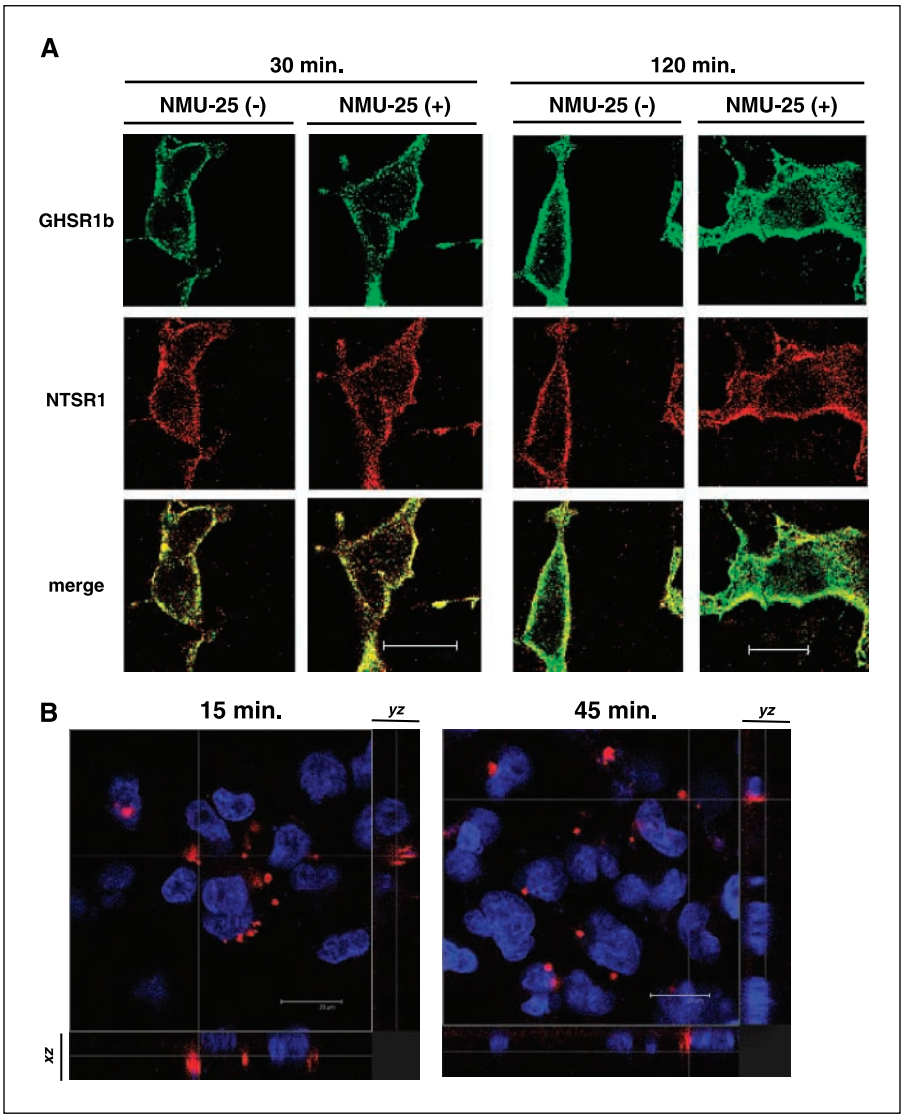

Figure 5. Characterization of GHSR1b/NTSR1 heterodimers and their internalization as cognate receptors for NMU. *A,* internalization of GHSR1b/NTSR1 protein induced by NMU-25. COS-7 cells transiently expressing both GHSR1b and NTSR1 were exposed to NMU-25 (10 μmol/L) for 30 minutes (*left*) or 120 minutes (*right*). COS-7 cells without exposure to the NMU-25 treatment served as controls. Cells were subsequently fixed and stained using secondary antibodies conjugated to Alexa Fluor 488–labeled anti-GHSR antibody or Alexa Fluor 594–labeled anti-NTSR1 antibody. Subcellular distribution of the two receptor proteins was examined by confocal microscopy. *Bottom,* LC319 cells expressing both endogenous GHSR1b and NTSR1 were exposed to NMU-25 (10 μmol/L) for 30 minutes (*left*) or 120 minutes (*right*). *B,* internalization of NMU-25-Alexa 594 in LC319 cells. The cells were incubated with 35 μmol/L of NMU-25-Alexa 594 for 15 minutes (*left*) or 45 minutes (*right*) at 37°C, and subsequently washed and fixed. *Red,* NMU-25-Alexa 594; *blue,* cell nuclei (with DAPI). The *xz*- and *yz*-projections proved that the ligands were localized within the cells. *Dotted lines,* where the *xz*- and *yz*-projections were taken.

NTSR1 heterodimer was implied to be the possible targets for the growth-promoting effect of NMU in lung tumors. GHSR is a known receptor of GHRL, a recently identified 28–amino acid peptide capable of stimulating the release of pituitary growth hormone and appetite in humans (23, 36, 37). Of the two transcripts known to be receptors for GHRL, GHSR1a and GHSR1b, we detected overexpression of only *GHSR1b* in NSCLC tissues and cell lines. In NSCLC, GHRL was not significantly expressed in the cell lines examined (Fig. 4*A*), therefore, we suspected that GHSR1b could have a growth-promoting function in lung tumors through binding to NMU, but not to GHRL. Interestingly, it was reported that *GHRL* and *GHSR1b*, but not *GHSR1a* genes were overexpressed in the erythroleukemic HEL cells, whose proliferation was regulated by des-acyl GHRL in an autocrine manner (38). NTSR1 is one of three receptors of NTS, a brain and gastrointestinal peptide that fulfills many central and peripheral functions (24). NTS modulates the transmission of dopamine and secretion of pituitary hormones, and exerts hypothermic and analgesic effects in the brain, whereas it functions as a peripheral hormone in the digestive tract and cardiovascular system. Others have reported that NTS is produced and secreted in several human cancers, including SCLCs (24). We detected the expression of *NTS* in 4 of the 15 NSCLC cell lines we

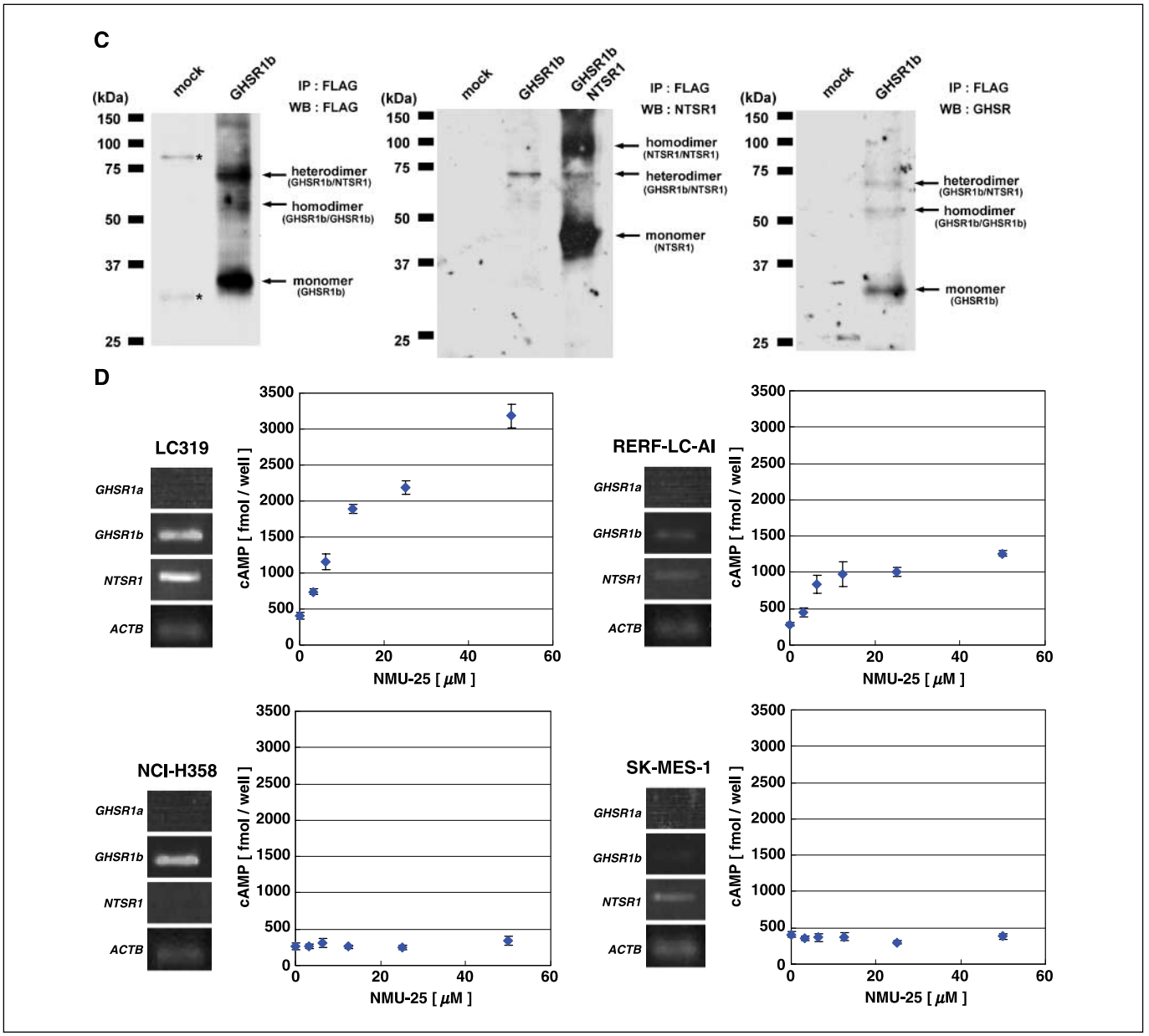

Figure 5 *Continued. C,* immunoprecipitation of cell lysates from COS-7 cells transiently expressed FLAG-tagged GHSR1b, and ones coexpressed both FLAG-tagged GHSR1b and NTSR1. The proteins immunoprecipitated by anti-FLAG antibody were subjected to SDS-PAGE and immunoblotted with anti-FLAG antibody (*left*), with anti-NTSR1 antibody (*middle*), or with anti-GHSR antibody (*right*). *Arrows,* monomers, heterodimers, and homodimers of the receptors. The molecular weight (kDa) markers are indicated on the left side of individual panels; *, nonspecific immunoreactive protein band detected by anti-FLAG antibody. *D,* relationship between the expression levels of GHSR1b/NTSR1 and intracellular cAMP production by NMU-25 in lung cancer cell lines. The expression levels of receptors in LC319, RERF-LC-AI, NCI-H358, and SK-MES-1 cells were detected by semiquantitative RT-PCR analysis. Dose-response curves of intracellular cAMP production by NMU-25 treatment (3-50 μmol/L) in individual cell lines are shown. All experiments were done in triplicate.

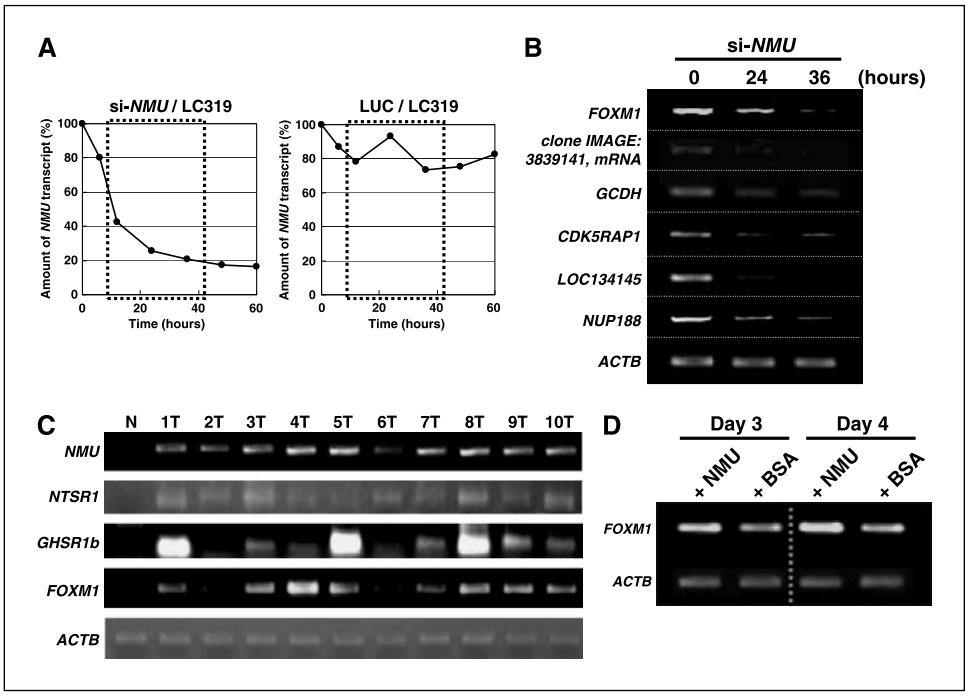

Figure 6. Identification of candidate downstream genes of the NMU signaling. *A,* time-dependent reduction of the *NMU* gene expression monitored by semiquantitative RT-PCR experiments of the mRNAs from LC319 cells treated with si-*NMU*, using *NMU*-specific primers. We prepared appropriate dilutions of each single-stranded cDNA prepared from mRNAs of LC319 cells at several time points. The β-actin (*ACTB*) expression was used as a quantitative control. Densitometric intensity of PCR product was quantified by image analysis software (Quantity One; Bio-Rad, Hercules, CA). *B,* time-dependent reduction of expression levels for possible target genes in the NMU signaling pathway was confirmed by semiquantitative RT-PCR experiments of mRNAs prepared from LC319 cells that were treated with si-*NMU*. Individual gene-specific primers were used for PCR amplification. *C,* expression of *NMU, NTSR1, GHSR1b*, and *FOXM1* in clinical NSCLC samples (*T,* lung tumor; *N,* normal lung tissue), examined by semiquantitative RT-PCR. *D,* induction of *FOXM1* expression in LC319 cells incubated with NMU-25, detected by semiquantitative RT-PCR using mRNAs prepared from LC319 cells treated with NMU-25 or BSA (as control; 25 μmol/L).

examined (Fig. 4*A*), but the expression pattern of *NTS* was not necessarily concordant with that of *NMU* or *NTSR1*. Therefore, we assume that NTS might contribute to the growth of NSCLC through NTSR1 or other receptor(s) in a small subset of NSCLCs.

In our experiments, the majority of the cancer cell lines and clinical NSCLCs that expressed NMU also expressed GHSR1b and NTSR1, indicating that these ligand-receptor interactions were likely to be involved in a pathway that is central to the growth-promoting activity of NMU in NSCLCs. *GHSR* and *NTSR1* were also expressed in COS-7 cells used to examine the growth and invasion effect of NMU; the data strongly supported the importance of these two receptors for oncogenesis. Our experiments further revealed that NMU-25 functionally bound to these receptors on the cell surface of NSCLC cells and subsequently induced the production of a second messenger, cAMP. We also showed that treatment of NSCLC cells with siRNAs for *GHSR* or *NTSR1* reduced the expression of these receptors and resulted in cancer growth inhibition. Elevated cAMP levels were generally observed via activation of adenylate cyclase, which activated protein kinase A (PKA). It was reported that GHRL did not displace ^{125}I-labeled rat NMU binding to NMU1R-expressing cells when tested at concentrations up to 10 mmol/L (39). However, GHRL or NTS competitively inhibited NMU-induced cAMP production in NSCLC cells.[8] Moreover, we provide biochemical and physiologic evidence for the internalization and heterodimerization of the two neuropeptide GPCRs, GHSR1b and NTSR1 (Fig. 5*A*; Supplementary Fig. S5). These results independently suggest that NMU stimulates NSCLC cell proliferation by a pathway through the GHSR1b-NTSR1 heterodimer whose function is quite different from the two known NMU-receptors, NMU1R and NMU2R. Heterodimerization has been shown to contribute to both ligand-binding affinity and signaling efficacy of GPCRs (40, 41). Heterodimers can be formed by receptors for various ligands/transmitters; for example, GPCRs for angiotensin and bradykinin (42), or those for opioid and adrenergic ligands (43). Moreover, it has been reported that coexpression of GHSR1a and GHSR1b resulted in an attenuation of the signaling capability of GHSR1a, suggesting that GHSR1b possibly interacted with GHSR1a through receptor heterodimerization (44). Based on the fact that GHSR1b exhibits no function towards GHRL (45), heterodimerization of GHSR1a and GHSR1b might in fact be a common feature for GHSR. The combination of our data with previous reports suggests that binding of NMU to GHSR1b/NTSR1 heterodimer, which cooperated with G proteins of the G_s subfamily, leads to the activation of adenylate cyclase, accumulation of intracellular cAMP, and activation of cAMP-dependent protein kinase (PKA), and that the subsequent release of catalytic subunits of PKA (C) from the regulatory subunits (R) activates downstream target genes, thus, finally resulting in the activation of growth-promoting pathways.

Microarray data of LC319 cells treated with siRNA for *NMU* suggests that the NMU signaling pathway could affect the growth promotion of lung cancer cells by transactivating a set of downstream genes. We provided evidence that the FOXM1 transcription factor is one of the downstream targets in the NMU signaling pathway. In our tissue microarray experiments, we observed that the expression pattern of FOXM1 was significantly concordant with that of NMU in the same set of tumors, and that lung cancer patients with FOXM1-positive tumors showed shorter survival periods than patients with FOXM1-negative tumors, thus, independently confirming the effect of NMU-FOXM1 signaling on the promotion of the malignant nature of lung cancer cells. FOXM1 was known to be overexpressed in several types of human cancers (46–48). We also confirmed that treatment of NSCLC cells with specific siRNA to reduce the expression of *FOXM1* resulted in growth suppression.[8] To predict the transcriptional regulation of the *FOXM1* gene by cAMP-response element (CRE)–binding protein, we also screened the CRE-like sequence within a 1-kb upstream region of the putative transcription start sequence using the computer prediction program and found that the region

[8] Unpublished data.

contains three CRE-like elements (data not shown). Moreover, it should be noted that the luciferase reporter gene assay suggested that two of the CRE-like sequences are essential for effective augmentation of *FOXM1* promoter activity following NMU stimulation.[8] We speculate that CRE-binding proteins phosphorylated by PKA might be directly responsible for the regulation of *FOXM1* expression. Previous reports suggested that some cyclin genes are possible transcription targets of FOXM1 transcription factor and that FOXM1 controls the transcription network of genes which are essential for cell division and exit from mitosis (29). In fact, we observed the activation of *CCNB1* and *CCNA2* in the majority of a series of clinical NSCLC we examined and its good concordance of the expression to *FOXM1* expression. These data indicate the possibility that the NMU-FOXM1 pathway is finally linked to cyclin-dependent pathways.

In summary, we have shown that NMU and the recently identified heterodimerization of GHSR1b and NTSR1 are likely to play an essential role for an autocrine growth-promoting pathway in NSCLCs by modulating the transcription of downstream target genes including *FOXM1*. The data reported here strongly imply the possibility of designing new anticancer drugs, specific for lung cancer, that target the NMU-GHSR1b/NTSR1 pathway as well as the development of novel diagnostic/prognostic markers for lung cancer.

Acknowledgments

Received 4/18/2006; revised 7/24/2006; accepted 8/4/2006.

Grant support: "Research for the Future" Program Grant of The Japan Society for the Promotion of Science (no. 00L01402) to Y. Nakamura.

The costs of publication of this article were defrayed in part by the payment of page charges. This article must therefore be hereby marked *advertisement* in accordance with 18 U.S.C. Section 1734 solely to indicate this fact.

References

1. Greenlee RT, Hill-Harmon MB, Murray T, Thun M. Cancer statistics. CA Cancer J Clin 2001;51:15–36.
2. Sozzi G. Molecular biology of lung cancer. Eur J Cancer 2001;37:63–73.
3. Schiller JH, Harrington D, Belani CP, et al. Comparison of four chemotherapy regimens for advanced non-small-cell lung cancer. N Engl J Med 2001;346:92–8.
4. Kikuchi T, Daigo Y, Katagiri T, et al. Expression profiles of non-small cell lung cancers on cDNA microarrays: identification of genes for prediction of lymph-node metastasis and sensitivity to anti-cancer drugs. Oncogene 2003;22:2192–205.
5. Kakiuchi S, Daigo Y, Ishikawa N, et al. Prediction of sensitivity of advanced non-small cell lung cancers to gefitinib (Iressa, ZD1839). Hum Mol Genet 2004;13:3029–43.
6. Suzuki C, Daigo Y, Kikuchi T, Katagiri T, Nakamura Y. Identification of COX17 as a therapeutic target for non-small cell lung cancer. Cancer Res 2003;63:7038–41.
7. Suzuki C, Daigo Y, Ishikawa N, et al. ANLN plays a critical role in human lung carcinogenesis through activation of RHOA and by involvement in PI3K/AKT pathway. Cancer Res 2005;65:11314–25.
8. Ishikawa N, Daigo Y, Yasui W, et al. ADAM8 as a novel serological and histochemical marker for lung cancer. Clin Cancer Res 2004;10:8363–70.
9. Ishikawa N, Daigo Y, Takano A, et al. Increases of amphiregulin and transforming growth factor-α in serum as predictors of poor response to gefitinib among patients with advanced non-small cell lung cancers. Cancer Res 2005;65:9176–84.
10. Kato T, Daigo Y, Hayama S, et al. A novel human tRNA-dihydrouridine synthase involved in pulmonary carcinogenesis. Cancer Res 2005;65:5638–46.
11. Furukawa C, Daigo Y, Ishikawa N, et al. PKP3 oncogene as prognostic marker and therapeutic target for lung cancer. Cancer Res 2005;65:7102–10.
12. Minamino N, Kangawa K, Matsuo H. Neuromedin U-8 and U-25: novel uterus stimulating and hypertensive peptides identified in porcine spinal cord. Biochem Biophys Res Commun 1985;130:1078–85.
13. Domin J, Ghatei MA, Chohan P, Bloom SR. Characterization of neuromedin U-like immunoreactivity in rat, porcine, guinea-pig and human tissue extracts using a specific radioimmunoassay. Biochem Biophys Res Commun 1986;140:1127–34.
14. Domin J, Yiangou YG, Spokes RA, et al. The distribution, purification, and pharmacological action of an amphibian neuromedin U. J Biol Chem 1989;264:20881–5.
15. Kage R, O'Harte F, Thim L, Conlon JM. Rabbit neuromedin U-25: lack of conservation of a posttranslational processing site. Regul Pept 1991;33:191–8.
16. Austin C, Oka M, Nandha KA, et al. Distribution and developmental pattern of neuromedin U expression in the rat gastrointestinal tract. J Mol Endocrinol 1994;12:257–63.
17. Fujii R, Hosoya M, Fukusumi S, et al. Identification of neuromedin U as the cognate ligand of the orphan G protein-coupled receptor FM-3. J Biol Chem 2000;275:21068–74.
18. Howard AD, Wang R, Pong SS, et al. Identification of receptors for neuromedin U and its role in feeding. Nature 2000;406:70–4.
19. Funes S, Hedrick JA, Yang S, et al. Cloning and characterization of murine neuromedin U receptors. Peptides 2002;23:1607–15.
20. Chin SF, Daigo Y, Huang HE, et al. A simple and reliable pretreatment protocol facilitates fluorescent *in situ* hybridisation on tissue microarrays of paraffin wax embedded tumour samples. Mol Pathol 2003;56:275–9.
21. Callagy G, Cattaneo E, Daigo Y, et al. Molecular classification of breast carcinomas using tissue microarrays. Diagn Mol Pathol 2003;12:27–34.
22. Kohonen T. The self-organizing map. Proc IEEE 1990;78:1464–80.
23. Kojima M, Hosoda H, Date Y, Nakazato M, Matsuo H, Kangawa K. Ghrelin is a growth-hormone-releasing acylated peptide from stomach. Nature 1999;402:656–60.
24. Heasley LE. Autocrine and paracrine signaling through neuropeptide receptors in human cancer. Oncogene 2001;20:1563–9.
25. Bohm SK, Grady EF, Bunnett NW. Regulatory mechanisms that modulate signalling by G-protein-coupled receptors. Biochem J 1997;322:1–18.
26. Koenig JA, Edwardson JM. Endocytosis and recycling of G protein-coupled receptors. Trends Pharmacol Sci 1997;18:276–87.
27. Ghinea N, Vu Hai MT, Groyer-Picard MT, Houllier A, Schoevaert D, Milgrom E. Pathways of internalization of the hCG/LH receptor: immunoelectron microscopic studies in Leydig cells and transfected L-cells. J Cell Biol 1992;118:1347–58.
28. Vandenbulcke F, Nouel D, Vincent JP, Mazella J, Beaudet A. Ligand-induced internalization of neurotensin in transfected COS-7 cells: differential intracellular trafficking of ligand and receptor. J Cell Sci 2000;113:2963–75.
29. Faure MP, Alonso A, Nouel D, et al. Somatodendritic internalization and perinuclear targeting of neurotensin in the mammalian brain. J Neurosci 1995;15:4140–7.
30. Austin C, Nandha KA, Meleagros L, Bloom SR. Cloning and characterization of the cDNA encoding the human neuromedin U precursor: NMU expression in the human gastrointenstinal tract. J Mol Endocrinol 1995;14:157–69.
31. Ivanov TR, Lawrence CB, Stanley PJ, Luckman SM. Evaluation of neuromedin U actions in energy homeostasis and pituitary function. Endocrinology 2002;143:3813–21.
32. Hanada R, Teranishi H, Pearson JT, et al. Neuromedin U has a novel anorexigenic effect independent of the leptin signaling pathway. Nat Med 2004;10:1067–73.
33. Steel JH, Van Noorden S, Ballesta J, et al. Localization of 7B2, neuromedin B, and neuromedin U in specific cell types of rat, mouse, and human pituitary, in rat hypothalamus, and in 30 human pituitary and extrapituitary tumors. Endocrinology 1988;122:270–82.
34. Shetzline SE, Rallapalli R, Dowd KJ, et al. Neuromedin U: a Myb-regulated autocrine growth factor for human myeloid leukemias. Blood 2004;104:1833–40.
35. Euer NI, Kaul S, Deissler H, Mobus VJ, Zeillinger R, Weidle UH. Identification of L1CAM, Jagged2 and Neuromedin U as ovarian cancer-associated antigens. Oncol Rep 2005;13:375–87.
36. Kim K, Arai K, Sanno N, Osamura RY, Teramoto A, Shibasaki T. Ghrelin and growth hormone (GH) secretagogue receptor (GHSR) mRNA expression in human pituitary adenomas. Clin Endocrinol (Oxf) 2001;54:759–68.
37. Lambert PD, Anderson KD, Sleeman MW, et al. Ciliary neurotrophic factor activates leptin-like pathways and reduces body fat, without cachexia or rebound weight gain, even in leptin-resistant obesity. Proc Natl Acad Sci U S A 2001;98:4652–7.
38. De Vriese C, Gregoire F, De Neef P, Robberecht P, Delporte C. Ghrelin is produced by the human erythroleukemic HEL cell line and involved in an autocrine pathway leading to cell proliferation. Endocrinology 2005;146:1514–22.
39. Kojima M, Haruno R, Nakazato M, et al. Purification and identification of neuromedin U as an endogenous ligand for an orphan receptor GPR66 (FM3). Biochem Biophys Res Commun 2000;276:435–8.
40. Bouvier M. Oligomerization of G-protein-coupled transmitter receptors. Nat Rev Neurosci 2001;2:274–86.
41. Devi LA. Heterodimerization of G-protein-coupled receptors: pharmacology, signaling and trafficking. Trends Pharmacol Sci 2001;22:532–7.
42. AbdAlla S, Lother H, Quitterer U. AT1-receptor heterodimers show enhanced G-protein activation and altered receptor sequestration. Nature 2000;407:94–8.
43. Rocheville M, Lange DC, Kumar U, Patel SC, Patel RC, Patel YC. Receptors for dopamine and somatostatin: formation of hetero-oligomers with enhanced functional activity. Science 2000;288:154–7.
44. Chan CB, Cheng CH. Identification and functional characterization of two alternatively spliced growth hormone secretagogue receptor transcripts from the pituitary of black seabream *Acanthopagrus schlegeli*. Mol Cell Endocrinol 2004;214:81–95.
45. Howard AD, Feighner SD, Cully DF, et al. A receptor in pituitary and hypothalamus that functions in growth hormone release. Science 1996;273:974–7.
46. Teh MT, Wong ST, Neill GW, Ghali LR, Philpott MP, Quinn AG. FOXM1 is a downstream target of Gli1 in basal cell carcinomas. Cancer Res 2002;62:4773–80.
47. van den Boom J, Wolter M, Kuick R, et al. Characterization of gene expression profiles associated with glioma progression using oligonucleotide-based microarray analysis and real-time reverse transcription-polymerase chain reaction. Am J Pathol 2003;163:1033–43.
48. Kalinichenko VV, Major ML, Wang X, et al. Foxm1b transcription factor is essential for development of hepatocellular carcinomas and is negatively regulated by the p19ARF tumor suppressor. Genes Dev 2004;18:830–50.

The Neuromedin U-Growth Hormone Secretagogue Receptor 1b/Neurotensin Receptor 1 Oncogenic Signaling Pathway as a Therapeutic Target for Lung Cancer

Koji Takahashi, Chiyuki Furukawa, Atsushi Takano, et al.

Cancer Res 2006;66:9408-9419.